JOURNAL OF CATALYSIS 155, 32–42 (1995)

# Deactivation and Compound Formation in Sulfuric Acid Catalysts and Model Systems

K. M. Eriksen,* D. A. Karydis,† S. Boghosian,† and R. Fehrmann*,[1]

*Chemistry Department A, Building 207, The Technical University of Denmark, DK-2800 Lyngby, Denmark; and †Institute of Chemical Engineering and High Temperature Chemical Processes, and Department of Chemical Engineering, University of Patras, P.O. Box 1414, GR-26500 Patras, Greece

Received August 4, 1994; revised February 28, 1995

**The catalytic deactivation and the simultaneous formation of compounds in industrial sulfuric acid catalysts and their molten salt–gas model systems $M_2S_2O_7/V_2O_5$–$SO_2/O_2/SO_3/N_2$ ($M$ = Na, K, Cs) have been studied by combined activity measurements and *in situ* ESR spectroscopy at temperatures up to 500°C. The applied gas compositions were unconverted, and 50 and 90% preconverted standard feed gas containing 10% $SO_2$, 11% $O_2$, and 79% $N_2$. This covers the conditions of all beds in an industrial $SO_2$ converter, without interstage absorption of $SO_3$. The temperature of deactivation was shown to decrease with increased degree of preconversion of the feed gas, increased mixing of the alkali promoters, and decreased vanadium content in the catalysts and model systems. The precipitation of V(III), V(IV), and mixed valence V(IV)–V(V) compounds was observed below the onset temperature of the catalyst deactivation. The salts have been isolated under operating conditions from model melts and identified by microscopy and spectroscopic methods. The V(IV) compounds were characterized by ESR spectroscopy and their temperature of decomposition was found to be in the range 450–500°C. Based on the characteristic ESR spectra, the V(IV) compounds causing the deactivation of working industrial catalysts could be identified *in situ*. Finally it was found that the restoration of deactivated catalysts requires heating to around 500°C, where the low-valence vanadium compounds decompose and reoxidize to V(V).** © 1995 Academic Press, Inc.

## INTRODUCTION

The catalyst used for sulfuric acid production, catalyzing the reaction $SO_2 + \frac{1}{2}O_2 \rightarrow SO_3$, is a supported liquid phase (SLP) catalyst, usually made by calcination of diatomaceous earth, vanadium pentoxide (or other V salts), and alkali salt promoters (usually in the form of sulfates) with the alkali-to-vanadium molar ratio ranging from 2 to 5. During the activation process, large quantities of sulfur oxides are taken up by the catalyst, forming molten alkali pyrosulfates (1, 2) which dissolve the vanadium salts. Thus, the molten salt–gas system $M_2S_2O_7/V_2O_5$–$SO_2/O_2/SO_3/N_2$ ($M$ = Na, K, Cs) at 400–600°C is considered to be a realistic model of the working industrial catalyst. A major problem in the $SO_2$ oxidation process is the sudden drop in activity which is experienced in all commercial catalysts at an operating temperature below ~420°C. Interstage (and costly) absorption of $SO_3$ before the last catalyst bed has thus become unavoidable in order to attain low $SO_2$ content in the stack gas.

Previously (3, 4) very little has been known about complex and compound formation in the catalyst. However, this fundamental knowledge is essential for the understanding of the unknown reaction mechanism and the severe deactivation of the catalyst below ~420°C. Unfortunately, a direct study of the species formed in the liquid phase, which is dispersed in the small pores of the industrial catalyst, is very difficult and probably only methods like ESR and NMR can be applied. The present paper is a part of an ongoing study dealing with (i) the complex and redox chemistry of vanadium; (ii) the formation of V(III), V(IV), and V(V) compounds; and (iii) the physicochemical properties of the catalyst model system (5–7 and references therein). The project strategy is to study both the working industrial catalysts and model systems in order to check if their chemistries can be linked together. Studies of $SO_2$ oxidation in unsupported $V_2O_5$–$M_2S_2O_7$ molten salt model systems (5) allow the isolation of precipitating V(IV) and V(III) crystalline compounds below the temperature of the well-known (3, 8, 10–13) break in the Arrhenius plots of the apparent reaction rates. In this way, the compounds $K_4(VO)_3(SO_4)_5$, $Na_2VO(SO_4)_2$, $Cs_2(VO)_2(SO_4)_3$, $KV(SO_4)_2$, $NaV(SO_4)_2$, and $CsV(SO_4)_2$ have been identified as deactivation products (5). However, *in situ* investigations of the vanadium complex formation and the compound formation during deactivation of industrial catalysts are essentially missing. Thus a preliminary study by some of the authors (9) of a commercial sulfuric acid catalyst in unconverted 10% $SO_2$, 11% $O_2$, and 79% $N_2$ feed gas demonstrated by *in situ* ESR that

[1] To whom correspondence should be addressed.



0021-9517/95 $12.00

the V(IV) compound $K_4(VO)_3(SO_4)_5$ precipitated at and below the onset temperature of the deactivation. In this way the catalyst melt was depleted for the dissolved active vanadium complexes. In addition, only the old studies of Boreskov *et al.* (10, 11) of a catalyst which is no longer produced can be found in the literature. The spectra are rather poor and no conclusion could be made on the possible compounds formed at lower temperatures, also due to the lack of relevant reference compounds. In addition, only two *in situ* ESR investigations of model melts supported on CPG (controlled pore glass) have been published so far; one study (14) dealing with K- and Cs-promoted melts gave very poor spectra and uncertain conclusions and the other (7) was concerned with model melts rather dilute in vanadium compared to industrial catalysts.

However, the previous investigations of the industrial catalysts and molten salt model systems (5, 9) were performed using only unconverted feed gas, i.e., 10% $SO_2$, 11% $O_2$, and 79% $N_2$, reflecting the conditions in the first bed of an industrial converter. The present study involves both unconverted as well as 50 and 90% preconverted feed gases, thus simulating the conditions in all catalyst beds. The 90% preconverted gas, i.e., 1% $SO_2$, 9% $SO_3$, 7% $O_2$, and 83% $N_2$, corresponds to the composition of the mixture that would enter the last bed of a one-stream converter without interstage absorption of $SO_3$. Such a setup is desired for technical and economical reasons and a study of the catalyst chemistry under these conditions might be important for the design of industrial catalysts with sufficiently improved activity below ~420°C.

## EXPERIMENTAL

### *Chemicals*

The $K_2S_2O_7$ and $Na_2S_2O_7$ used were made by thermal decomposition of $K_2S_2O_8$ (Merck, pro analysi) and $Na_2S_2O_8$ (Fluka, pro analysi) as previously described (15) and were stored in sealed ampoules. $Cs_2S_2O_8$ is not commercially available and it was synthesized as previously (16), and decomposed to $Cs_2S_2O_7$ at 300°C in a stream of nitrogen. $V_2O_5$ was from Cerac (pure, >99.9%). All handling of the chemicals and filling of cells were performed in nitrogen-filled dry boxes with a water content of 1–5 ppm.

The controlled pore glass (CPG) support was from CPG Inc. (pore size: 50–90 nm for >99%). The industrial catalysts were from Haldor Topsøe A/S, Denmark: VK-38 (ca. 6% $V_2O_5$ on kieselguhr, $M/V$ = 3.8 (K/Na/V = 3/0.8/1)) and VK-58 (ca. 7% $V_2O_5$ on kieselguhr, $M/V$ = 4.25 (K/Cs/Na/V = 3/1/0.25/1)).

Commercial gases $SO_2$(>99.9%), $O_2$ (99.8% $O_2$ + 0.2% $N_2$ and Ar), and $N_2$ (<40 ppm $O_2$ + $H_2O$) were used.

### *Catalytic Activity Measurements*

The gas–molten salt reactor system used has been described in detail elsewhere (5). The $SO_2$, $O_2$, and $N_2$ streams were passed through moisture and hydrocarbon traps and mixed by means of mass flow controllers. A Pt-catalyst-based preconverter and a $SO_2$ bypass stream were used so that any $SO_2/SO_3/O_2/N_2$ mixture could be achieved and the degree of preconversion and/or the conversion through the reactor was determined by gas chromatographic detection of $SO_2$ after the $SO_3$ has been absorbed in a 96% sulfuric acid solution or condensed in a cold trap at −35°C.

The reactor cell containing the $V_2O_5$–$M_2S_2O_7$ molten salt mixtures or the industrial catalysts studied has also been described earlier (5). The cell design allowed us to observe visually the formation of crystalline precipitates and allowed their isolation under operating conditions.

The gas chromatograph was a Shimadzu GC 9A with a thermal conductivity detector and two 0.32-cm o.d. and 2.4-m-long stainless-steel columns packed with Porapak Q (80–100 mesh). The GC was equipped with a uniformly heated 80°C Valco 6-port external gas sampling valve possessing a 2-ml loop. The carrier gas was He, and the column and detector temperatures were set at 100 and 85°C, respectively. The GC was operated isothermally. A Perkin–Elmer LCI-100 computing integrator was used for integrating the chromatographic peak areas.

All piping was made of stainless steel, glass, or flexible Viton rubber tubing in order to minimize corrosion and was wrapped with heating tape (heated to ~80°C) to prevent condensation of $SO_3$.

Catalytic activity of the industrial catalysts and model melts was determined as the steady-state turnover frequency (i.e., as mol $SO_2$ converted/mol V/s. The space velocity was varied in the range 5000–10,000 $h^{-1}$ in such a way that the conversion across the reactor was sufficiently low (<15%) for the reactor to be considered differential.

### *ESR Spectroscopy*

The synthesis gas (which was premixed in a steel bottle) consisting of 10% $SO_2$, 11% $O_2$, and 79% $N_2$ was passed through a moisture trap (granulated $P_2O_5$) and fed to a preconverter before entering the ESR reactor cell. The temperature of the preconverter was chosen so that the thermodynamically controlled position of the equilibrium $SO_2 + \frac{1}{2}O_2 \rightleftarrows SO_3$ fitted to the desired gas composition. The ESR reactor cell has previously been described in detail (9). It consists of two thin (~0.1 mm in thickness) concentric quartz tubes, 1.5 and 2 mm in diameter, respectively. The inner tube contains the gently crushed catalyst sample, up to around 35 mg, and a small separate ruby crystal which allows one to correct the signal intensity for the temperature dependence. Field calibration was

performed by means of a Mn(II) standard. The temperature was measured by a 1-mm Chromel/constantan thermocouple (not magnetic) placed on top of the sample. When the reactor cell was introduced into the Dewar vessel of the high-temperature cavity, only the lower 2 cm was situated in the sensitive zone of the cavity. The gas entered the outer tube and was thus heated before passing into the inner tube where the sample was placed in a bed between two plugs of quartz wool. The space velocity of the gas was adjusted so that the conversion of $SO_2$ across the catalyst bed was less than 5%, assuring a uniform catalyst sample during the measurements. Analysis of the gas composition was made by chromatographic detection of $SO_2$, as in the case of the catalytic activity measurements. All 1/8" stainless steel tubes of the experimental setup were heated to 80–90°C with wrapped heating tape in order to prevent possible condensation of $SO_3$.

In order to ensure that a steady state was attained, the ESR spectra were followed as a function of time until a stable signal was obtained and were recorded typically 2 h after adjusting the process parameters (gas compositions, temperature).

## RESULTS AND DISCUSSION

### *Catalytic Activity of Catalysts and Model Melts*

The catalytic activities of industrial catalysts and $M_2S_2O_7$–$V_2O_5$ model melts containing the various alkali promoters ($M$ = Na, K, and Cs) with $M$/V molar ratios between 3 and 10 have been measured in the temperature range 360–480°C, i.e., covering the regions of both high and low catalytic activity. A 5% $SO_2$, 5% $SO_3$, 9% $O_2$, and 81% $N_2$ mixture was used as the feed gas, i.e., corresponding to 50% conversion of the 10% $SO_2$, 11% $O_2$, and 79% $N_2$ gas mixture that typically enters the first stage of an industrial converter. Thus the measurements reflected conditions similar to those of the second catalyst bed. The conversion was stable as measured by GC at each temperature after 2–12 h, indicating that steady state has been obtained. The results are displayed in Figs. 1 and 2. Two regions with low and high activation energy, respectively, are observed, crossing each other in a sharp break at a temperature $T_b$, given in Table 1. In the high-temperature region ($T > T_b$) the catalyst model systems are liquid while formation of crystalline solids occurs below $T_b$. As temperature is gradually reduced, increasing amounts of precipitate are accumulated. However, in the case of the Na-promoted model melts with the highest V content, i.e., Na/V = 3 and 4.7, a crystalline phase is already observed at the highest measuring temperature. Blue V(IV) and green V(III) salts were isolated from the melts either by filtration at high temperatures (performed by reversing the flow through the reactor cell) as described in Ref. (5) or from the solidified mixture, by flushing the cell with water after interrupting the experiment. In this way, the low-soluble V(IV) compounds $Na_2VO(SO_4)_2$, $K_4(VO)_3(SO_4)_5$, and $Cs_2(VO)_2(SO_4)_3$ and V(III) compounds $NaV(SO_4)_2$, $KV(SO_4)_2$, and $CsV(SO_4)_2$ were isolated as previously (5) and identified by microscopy and/or ESR and IR spectroscopy. Thus at temperatures below $T_b$ the liquid phase of the catalyst is gradually depleted for active dissolved vanadium species, which are precipitated in the form of the above-mentioned compounds. Finally, at the liquidus temperature defined by the $M_2S_2O_7$–$V_2O_5$ phase diagrams (16–18), V(V) compounds also precipitate.

The results of the present and previous (5) investigations are compared in Table 1. The apparent activation energies, obtained from the slopes of the lines in the Arrhenius-type plots given in Fig. 1, are comparable for the two different gas compositions. However, the break in these plots is shifted to lower temperatures for the melts in the 50% preconverted gas. This is probably due to a

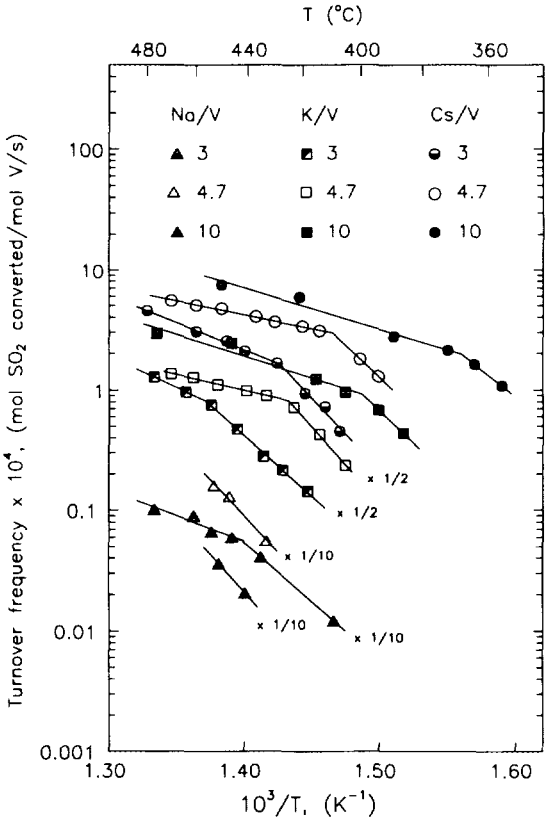


FIG. 1. Arrhenius plots of measured reaction rates for alkali-promoted catalyst model melts. Feed gas: 5% $SO_2$, 5% $SO_3$, 9% $O_2$, and 81% $N_2$ ($x_p$ = 0.5): Triangles, squares, and circles refer to Na-, K-, and Cs-promoted catalyst melts, respectively. The alkali-to-vanadium mole ratio is as indicated in the figure. For clarity, some plots have been reduced by the indicated factor.

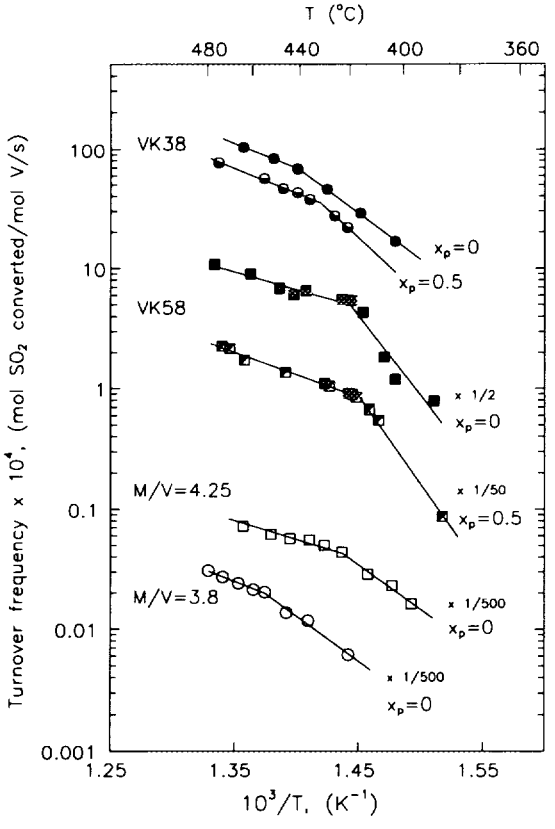


FIG. 2. Arrhenius plots of measured reaction rates for the mixed alkali-promoted industrial catalysts VK-38 (Na, K) and VK-58 (Na, K, Cs) and their model melts. Feed gas: 10% $SO_2$, 11% $O_2$, and 79% $N_2$ ($x_p$ = 0) or 5% $SO_2$, 5% $SO_3$, 9% $O_2$, and 81% $N_2$ ($x_p$ = 0.5). Circles refer to VK-38 and squares to VK-58. The open symbols indicate the catalyst model melts, with the total alkali-to-vanadium molar ratios $M$/V = 3.8 (VK-38) and $M$/V = 4.25 (VK-58), respectively. For clarity, some plots have been reduced by the indicated factor.

shift of the formal equilibria system

$$V(V) \underset{SO_3}{\overset{SO_2}{\rightleftarrows}} V(IV) \underset{SO_3}{\overset{SO_2}{\rightleftarrows}} V(III) \qquad [1]$$

to the left, since the partial pressure ratio $P_{SO_3}/P_{SO_2}$ is larger compared to the unconverted feed gas. Thus the critical concentration (the solubility limit) of V(IV) and V(III) is achieved at lower temperatures in the 50% preconverted gas and $T_b$ is accordingly lower. Indeed, recent spectrophotometric and ESR measurements on dilute solutions of $V_2O_5$ in molten pyrosulfates (7) show that the V(V)–V(IV) redox equilibrium is shifted toward V(IV) as the temperature is lowered. Furthermore, the type of alkali promoter seems to influence the position of the redox equilibria. Thus it is known that increasing the radius of the alkali metal ion, i.e., in the sequence Li, Na, K, Rb, Cs, increases the ability of their sulfates to absorb $SO_3$ (forming pyrosulfate and higher pyrosulfates) and stabilize the vanadium in the +5 oxidation state (19–21). This trend is in accordance with the observed decrease in $T_b$ for the Na- K-, and Cs-based model melts, respectively, with the same molar ratio $M$/V (Table 1), but other factors, such as differences in the solubility product of the precipitating salts, may also be significant. In the case of supported catalysts the pore size distribution also has a significant influence (3). Furthermore, from Fig. 1 and Table 1 it is seen that an increase in the $M$/V ratio in series 3, 4.7, 10 leads in all cases to a decrease in $T_b$. This is presumably due to a simple dilution effect but probably also due to increasing activity of $S_2O_7^{2-}$ in the melts through this row, shifting the redox equilibria toward V(V).

The behavior of the industrial catalysts is very similar to that of their model melts as can be seen in Fig. 2. Thus VK-38 with the molar ratio $M$/V = 3.8 ($M$ = 80% K + 20% Na) has $T_b$ values in good agreement with the model melt for $x_p$ = 0, and between the K/V = 3 and 4.7 model melts for $x_p$ = 0.5. The VK-58 catalyst has a molar ratio $M$/V = 4.25 ($M$ = 70% K + 25% Cs + 5% Na) and it deactivates at nearly the same temperature as the model melt for $x_p$ = 0. The activity loss of this catalyst occurs at lower temperatures compared to both VK-38 and the K/V = 4.7 melt for both feed gases used. This is probably due to the mixture of all three cations in VK-58, which leads to a higher solubility of the individual alkali V(IV) and V(III) salts moving $T_b$ toward lower values, as discussed previously (5). VK-38 has a chemical composition common for other commercial catalysts, while VK-58, with Cs, has been developed recently.

Indeed, Cs-promoted catalysts have been shown (13) to have lower $T_b$ than analogous catalysts promoted by K. In addition, and also in accordance with our results for model melts, it was also shown that $T_b$ was lowered by increasing the Cs/V molar ratio for Cs-promoted catalysts through the row Cs/V = 2.5, 3, 3.5 (13). The apparent activation energies above and below the deactivation temperature (Table 1) are in good agreement with previous investigations on model melts and supported catalysts (5, 12, 13, 22–24).

As previously stated (5), it should be noted that the catalytic activities displayed in Fig. 1 are only relative and not the highest attainable.

Attempts to measure the catalytic activity and deactivation in 90% preconverted gas ($x_p$ = 0.9) failed because of too high an uncertainty in the GC measurements due to poor stability of the flowmeter for the very small $SO_2$ bypass stream. However, these measurements could be carried out in the ESR investigation.

*ESR Spectra of V(IV) Compounds*

The room-temperature ESR powder spectra of the three V(IV) compounds and of $\beta$-$VOSO_4$, isolated from model

TABLE 1

**Temperature of the Activity Drop and Apparent Activation Energies of the Catalyst Melts[a]**

| Model melt or catalyst | $T_b$[b] (°C) | | Apparent activation energy (kcal/mol) | | | |
|---|---|---|---|---|---|---|
| | | | $x_p = 0$ | | $x_p = 0.5$ | |
| | $x_p = 0$ | $x_p = 0.5$ | $T > T_b$ | $T < T_b$ | $T > T_b$ | $T < T_b$ |
| Na/V = 3 | (>470)[c] | (>475)[c] | — | 49.2 | — | 57.0 |
| Na/V = 4.7 | (>460)[c] | (>460)[c] | — | 49.2 | — | 54.5 |
| Na/V = 10 | (>460)[c] | 442 | — | 55.0 | 19.0 | 45.0 |
| K/V = 3 | (>475)[c] | 454 | — | 47.0 | 23.5 | 46.3 |
| K/V = 4.7 | 439 | 425 | 17.6 | 49.2 | 12.0 | 58.0 |
| K/V = 10 | 404 | 399 | 15.4 | 47.6 | 16.3 | 49.0 |
| Cs/V = 3 | 430 | 427 | 17.8 | 41.4 | 20.6 | 55.0 |
| Cs/V = 4.7 | 416 | 409 | 16.0 | 42.1 | 11.0 | 48.4 |
| Cs/V = 10 | 388 | 368 | 14.6 | 40.9 | 16.0 | 40.6 |
| VK-38 | 441 | 431 | 18.6 | 35.6 | 19.2 | 43.8 |
| VK-58 | 420 | 416 | 13.0 | 61.6 | 17.0 | 60.9 |
| $M$/V = 3.8[d] | 454 | — | 18.5 | 34.6 | — | — |
| $M$/V = 4.25[e] | 423 | — | 14.3 | 34.2 | — | — |

[a] Feed gas composition: $x_p = 0$: 10% $SO_2$, 11% $O_2$, 79% $N_2$; $x_p = 0.5$: 5% $SO_2$, 5% $SO_3$, 9% $O_2$, 81% $N_2$. All values for $x_p = 0$, except for the lower three in the table, are from Ref. (5).

[b] $T_b$ is the temperature at which the compound precipitation and the break in the Arrhenius plots occur simultaneously.

[c] $T_b$ is above the highest measured temperature, given in parentheses.

[d] $M$ = 80% K + 20% Na.

[e] $M$ = 70% K + 25% Cs + 5% Na.

melts at $x_p = 0.5$ and 0.9, respectively, are shown in Fig. 3. The powder spectra appears to be of the usual axial symmetric type, which can be resolved by Lorentzian functions (25). In this way, the $g$ components, $g_\perp$ and $g_\parallel$, and the linewidths of the isotropic and anisotropic spectra given in Fig. 3 have been obtained. The spectrum of $K_4(VO)_3(SO_4)_5$ exhibits very weak anisotropy and it is therefore treated as isotropic. The parameters are the same as found in the preliminary investigation (9).

No ESR parameters could be found for $Cs_2(VO)_2(SO_4)_3$, $\beta$-$VOSO_4$, or $Na_2VO(SO_4)_2$ in the literature. However, spectra very similar to that of $Na_2VO(SO_4)_2$ have previously been obtained from an unknown compound isolated from a heated mixture of $V_2O_5$ and $Na_2S_2O_7$ (26) and from a similar experiment in an open container where the spectrum was erroneously attributed to a V(IV)–V(V) mixed valence compound (27). Indeed a mixed valence compound, probably $Na_3(VO)_2(SO_4)_4$, has very recently been isolated from the molten $Na_2S_2O_7$–$V_2O_5$ system treated with 90% preconverted synthesis gas, i.e., 1% $SO_2$, 9% $SO_3$, 7% $O_2$, and 83% $N_2$, but the ESR spectrum (28) is very different from that of $Na_2VO(SO_4)_2$.

To complete the series of ESR spectra of possible V(IV) compounds precipitating during deactivation of catalysts and model melts, the results of ongoing X-ray and spectroscopic investigations on $\beta$-$VOSO_4$-like compounds with trapped $SO_2$ and/or $SO_3$ molecules should also be included (29). In addition, the mixed valence V(IV)–V(V) compound $K_3(VO)_2(SO_4)_4$, isolated from K-based model melts in gases with high $SO_3$ content, should be considered, too. X-ray and spectroscopic characterization of this compound is in progress (30).

### *In Situ ESR Investigations*

ESR investigations of model melts dispersed on CPG and of the industrial catalysts have been performed in unconverted ($x_p = 0$) and 90% preconverted ($x_p = 0.9$) 10% $SO_2$, 11% $O_2$, and 79% $N_2$ feed gas. The temperature range studied covered the molten and solidified state of the catalyst and model melts. The pure catalyst support is ESR-silent (9). Only the paramagnetic [Ar] $3d^1$ V(IV) species is expected to be ESR-observable since V(V) ([Ar] $3d^0$) is diamagnetic and V(III) ([Ar] $3d^2$) is expected to

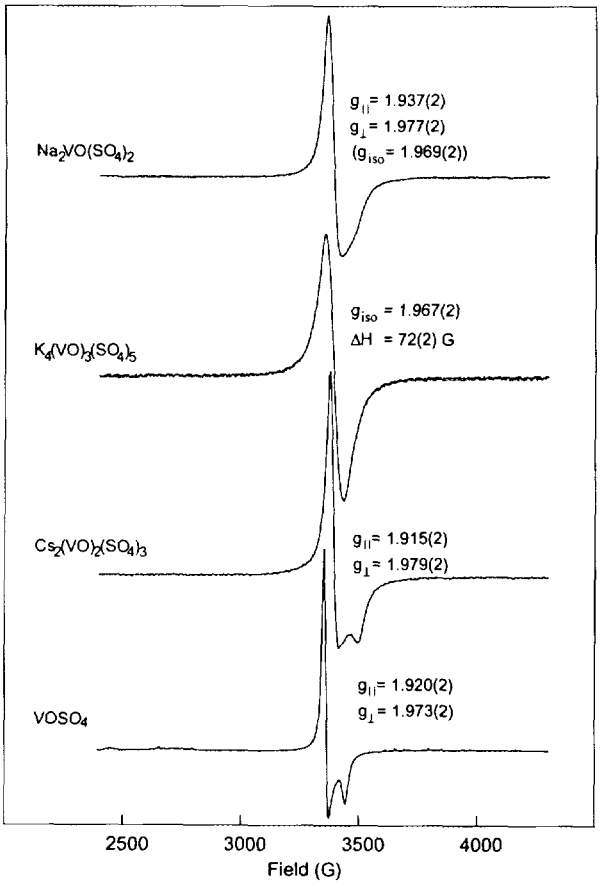


FIG. 3. ESR spectra of V(IV) compounds isolated from catalyst model melts. The isotropic $g$ values, anisotropic $g$ components, and the linewidth ($\Delta H$) are as indicated.

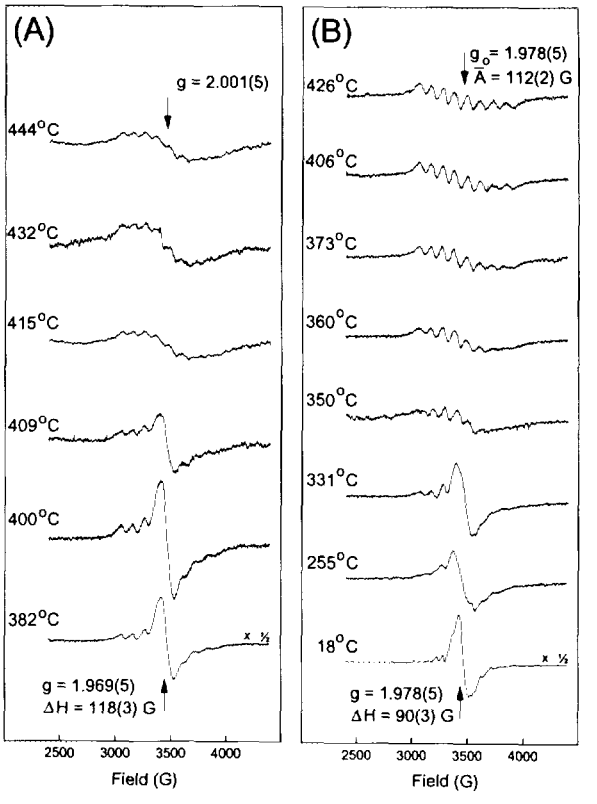


FIG. 4. ESR spectra of $K_2S_2O_7$–$V_2O_5$ melts with the molar ratio K/V = 8 in (A) 9% $SO_2$, 10% $O_2$, and 81% $N_2$ ($x_p$ = 0); (B) 1% $SO_2$, 8% $SO_3$, 7% $O_2$, and 84% $N_2$ ($x_p$ = 0.9). The isotropic $g$ values, hyperfine structure constant ($\bar{A}$), and the linewidths ($\Delta H$) are as indicated. For convenience, the signal intensity of the ESR spectra at the lowest temperatures have been reduced by the indicated factor.

resonate far from the field investigated here due to zero field splitting of the electronic spin states.

In Fig. 4 the spectra of 1 $M$ $V_2O_5$ in $K_2S_2O_7$ in both unconverted (A) and 90% preconverted gas (B) exhibit the same three-line features. At high temperature and especially at high conversion (B), the characteristic 8-line signal of monomeric vanadyl complexes is observed, arising from the coupling of the electron spin to the spin of the $^{51}V$ nucleus ($I$ = 7/2). In addition, and especially at low conversion (A), i.e., where the V(IV) concentration is relatively high, a broad apparently isotropic line is seen, too. This line is probably due to dimeric or polymeric V(IV) complexes where spin coupling to neighboring V atoms should give rise to multiline spectra. This has been observed previously (31–33) for dimeric V(IV) complexes at room temperature where a badly resolved 15-line spectra on a broad central line is found. This pattern is indeed expected to be even less resolved at elevated temperatures and for polymeric complexes, where long-range coupling might make the hyperfine structure undetectable. These isotropic signals are due to free rotating complexes in solution. At lower temperatures, a third relatively narrow anisotropic central line, characteristic of solid V(IV) compounds, appears in the spectra.

The $g$ value of 1.978(5) for the 8-line signal is identical to what was observed recently in more dilute solutions, i.e., 0.1 and 0.25 $M$ $V_2O_5$ in $K_2S_2O_7$ (7) and it is probably due to the vanadyl complex $VO(SO_4)_2^{2-}$. The broad line with a $g$ value of around 2.0 is probably due to a dimer/polymer V(IV) species, where the absence of hyperfine structure is due to long-range spin coupling. The possible monomer–polymer equilibrium $nVO(SO_4)_2^{2-} \rightleftarrows (VO(SO_4)_2)_n^{2n-}$ is expected to be shifted relatively more to the side of the monomer at low $P_{SO_2}$ and high $P_{SO_3}$ since the degree of reduction of V(V) to V(IV) decreases with increasing $P_{SO_3}/P_{SO_2}$ ratio (7). Thus the broad line of the polymer is very weak in the spectra at high conversion and the monomer signal is more pronounced. From these considerations, precipitation of V(IV) compounds is expected to appear at a higher temperature in unconverted gas. This is indeed the case where a V(IV) solid, most

probably $K_4(VO)_3(SO_4)_5$ (see Fig. 3), is formed at 409–415°C, compared to 331–350°C in the preconverted gas. In the latter case it appears to be the V(IV)–V(V) mixed valence compound $K_3(VO)_2(SO_4)_4$, as judged from the ESR spectra. The composition of these melts corresponds to the molar ratio K/V = 8. The temperature of precipitation, $T_p$, and the ESR parameters are listed in Table 2. The $T_p$ value can best be compared to the breakpoint temperature $T_b$ of the K/V = 10 melts given in Table 1. At low conversion ($x_p$), $T_p$ and $T_b$ are very close to each other, indicating that indeed $K_4(VO)_3(SO_4)_5$ is formed when the deactivation sets in. At high conversion ($x_p = 0.9$), $T_p$ is, as expected, lower than the $T_b$ found at intermediate conversion ($x_p = 0.5$).

The results of a similar investigation of the industrial catalyst VK-38 are shown in Fig. 5. As stated above, three types of signals are found both in unconverted (A) and 90% (B) preconverted gas. These are two isotropic lines, with and without hyperfine structure, and a strong narrow line at lower temperatures. In this case the 8-line signal of the monomeric complexes is relatively weak, especially at low conversion where it cannot be detected, compared to the broad line of the polymerized V(IV). However, the concentration of vanadium in the VK-38 catalyst ($M$/V = 3.8) is around 4 $M$, i.e., two times larger compared with the 1 $M$ $V_2O_5$ model melt studied above (Fig. 4), thus favoring polymerization. At lower temperatures sharp narrow lines appear in the spectra which can be attributed to the precipitation of $K_4(VO)_3(SO_4)_5$ and $\beta$-$VOSO_4$, respectively (Table 2). The $T_p$ value of 438–446°C for VK-38 in unconverted gas ($x_p = 0$) agrees very well with the temperature of deactivation, $T_b$, of 441°C given in Table 1 and with the previous ESR investigation (8). For $x_p = 0.9$, $T_p$ is found to be in the range 410–423°C, in good accordance with the trend for the $T_b$ values at $x_p = 0$ and 0.5 given in Table 1.

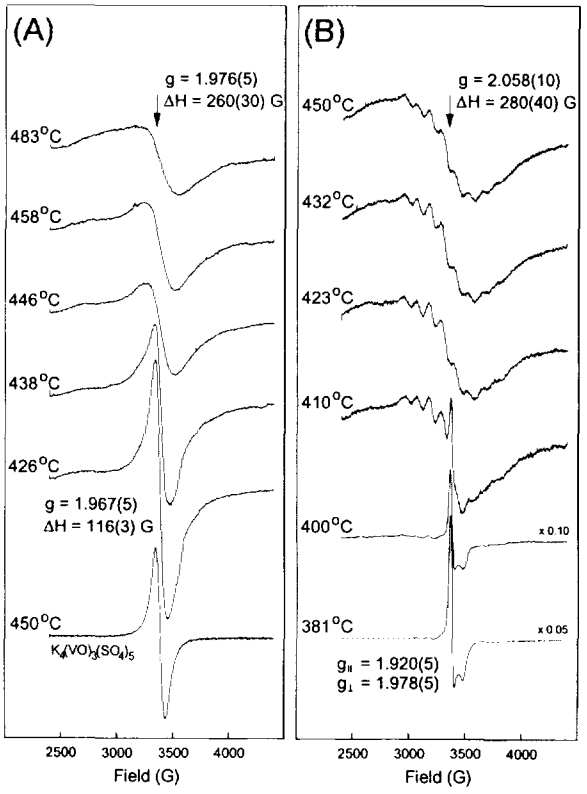


FIG. 5. ESR spectra of the catalyst VK-38 in (A) 10% $SO_2$, 11% $O_2$, and 79% $N_2$ ($x_p = 0$); (B) 1% $SO_2$, 9% $SO_3$, 7% $O_2$, and 83% $N_2$ ($x_p = 0.9$). The isotropic and anisotropic $g$ components and linewidths ($\Delta H$) are as indicated. For comparison, the spectrum of $K_4(VO)_3(SO_4)_5$ at 450°C is included. For convenience, the signal intensity of the spectra measured at the lowest temperatures in (B) have been reduced by the indicated factors.

TABLE 2

**ESR Investigations of Catalysts and Model Melts: Degree of Preconversion ($x_p$),[a] Temperatures of Precipitation ($T_p$), and ESR Parameters for the Solids**

| Catalyst or model melt | $x_p$ | $T_p$ (°C) | ESR parameters | | | | Most probable V(IV) compound formed during deactivation |
|---|---|---|---|---|---|---|---|
| | | | $g_\perp$ | $g_\parallel$ | $g_{iso}$ | $\Delta H$ (G) | |
| VK-38 | 0 | 438–446 | | | 1.967(5) | 116(3) | $K_4(VO)_3(SO_4)_5$ |
| VK-38 | 0.9 | 410–423 | 1.978(5) | 1.920(5) | | | $\beta$-$VOSO_4$ |
| VK-58 | 0 | 411–421 | | | 1.967(5) | 114(3) | $K_4(VO)_3(SO_4)_5$ |
| VK-58 | 0.9 | 398–406 | 1.980(5) | 1.919(5) | | | $\beta$-$VOSO_4$ or analogous compound[b] |
| K/V = 8[c] | 0 | 409–415 | | | 1.969(5) | 118(3) | $K_4(VO)_3(SO_4)_5$ |
| K/V = 8[c] | 0.9 | 331–350 | | | 1.978(5) | 90(3) | $K_3(VO)_2(SO_4)_4$[d] |

[a] Composition of unconverted gas: 10% $SO_2$, 11% $O_2$, 79% $N_2$.
[b] $VOSO_4$-like compound also containing $SO_2$ and/or $SO_3$ molecules, but no alkali metal ions (29).
[c] $K_2S_2O_7$–$V_2O_5$ melt on CPG.
[d] Mixed valence V(IV)–V(V) compound (30).

In one case the temperature was accidentally lowered suddenly from 443 to 415°C during an ESR investigation of VK-38 at $x_p = 0.9$ and, surprisingly, $K_4(VO)_3(SO_4)_5$ was formed instead of $\beta$-$VOSO_4$ (34). This illustrates how critical the kinetic parameters of crystallization might be for the compound formation.

The ESR spectra obtained on the Cs-, K-, and Na-promoted catalyst, VK-58, are shown in Fig. 6. Again the same type of signals are observed although the 8-line signal is not detected, i.e., the dissolved dimeric/polymeric V(IV) species dominates in the solution. As the temperature is lowered, a sharp, almost isotropic, signal and an anisotropic signal appear at low and high preconversion, respectively, which can be attributed to the precipitation of $K_4(VO)_3(SO_4)_5$ and $\beta$-$VOSO_4$ or an analogous compound with $SO_2$ and/or $SO_3$ molecules trapped in the crystal lattice (29). The precipitation temperature agrees well with the $T_b$ values given in Table 1. At both conversions and at low temperature a broad line on the low-field side of the compound signal is observed. This is probably caused by a frozen solution of the V(IV) polymer. In similar experiments a gradual decrease of this line at room temperature has been observed, presumably due to slow crystallization of the amorphous phase.

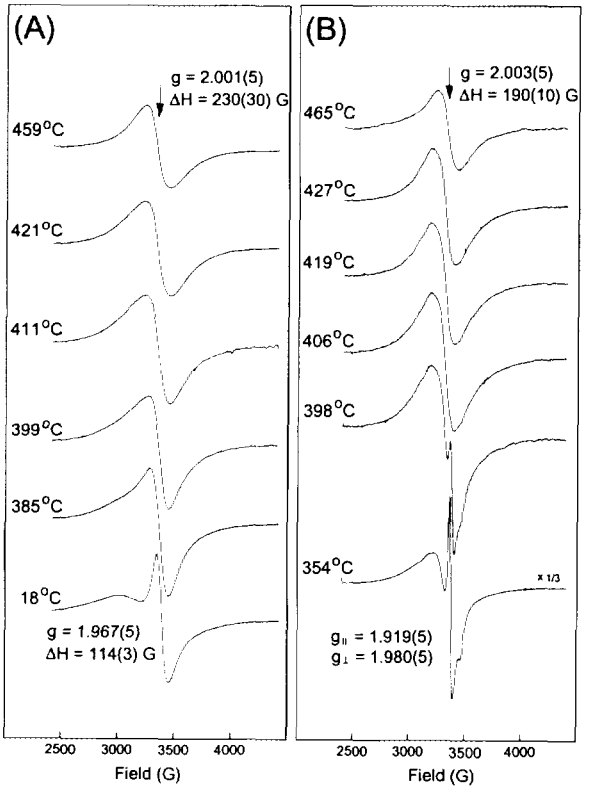


FIG. 6. ESR spectra of the catalyst VK-58 in (A) 10% $SO_2$, 11% $O_2$, and 79% $N_2$ ($x_p = 0$); (B) 1% $SO_2$, 9% $SO_3$, 7% $O_2$, and 83% $N_2$ ($x_p = 0.9$). The isotropic and anisotropic $g$ components and the linewidths ($\Delta H$) are as indicated. For convenience, the signal intensity of the spectrum measured at the lowest temperature in (B) has been reduced by the indicated factor.

Apparently, increasing $P_{SO_3}/P_{SO_2}$ ratio leads to the formation of compounds with less $SO_4^{2-}$ per $VO^{2+}$ unit, e.g., $\beta$-$VOSO_4$ is formed instead of $K_4(VO)_3(SO_4)_5$. This is probably due to a decreased activity of $SO_4^{2-}$ in the catalyst at high $P_{SO_3}$ in accordance with a shift of the solvent equilibrium,

$$SO_3 + SO_4^{2-} \rightleftarrows S_2O_7^{2-}, \qquad [2]$$

to the right.

In addition, the formation of compounds with less reduced vanadium, i.e., the mixed valence V(IV)–V(V) compounds, and the observation that no V(III) compounds thus far have been isolated from model melts in 90% preconverted gas, can be assigned to the increased $P_{SO_3}$, which shifts Eq. [1] to the left. The $T_p$ values for VK-58 are around 20°C lower than those found for VK-38 (Table 2) and probably caused by the "dilution" of K by the substituents Na and Cs, as discussed above. This property of VK-58 has made it attractive as a substitute for VK-38 in the last bed of industrial converters, which then can be operated at a lower temperature, leading to a higher overall conversion of $SO_2$. However, VK-58 is not sufficiently active below 400°C to eliminate the inconvenient interstage absorption of $SO_3$ before the last bed.

### *Temperature Stability of the V(IV) Compounds and Catalyst Reactivation*

It is well known that deactivated commercial catalysts can regain their activity by a heat treatment at 460–500°C and that the catalytic activity exhibits pronounced hysteresis (3, 35). This behavior is most probably due to a slow dissolution of the vanadium compounds precipitated in the pores of the catalyst carrier and probably in poor contact with the residual melt. Thus, the necessity of a heat treatment well above $T_b$ might be due to the oxidative decomposition of the precipitated, inactive V(III) and V(IV) compounds into melts with dissolved catalytically active complexes. Indeed, it has been shown by the previous ESR investigation (9) of VK-38 that heating of the deactivated catalyst to 492°C led to the disappearance of the signal from the solid, $K_4(VO)_3(SO_4)_5$, and to the reappearance of the signals from the dissolved V(IV) complexes. The previous combined activity, thermal, and IR spectroscopic investigation (5) also showed that the V(III) and V(IV) salts decompose presumably by $SO_2$ evolution to V(V) compounds at 470–500°C, leading to restoration of the catalytic activity.

The stability of the V(IV) compounds vs temperature has been studied by ESR spectroscopy in the present

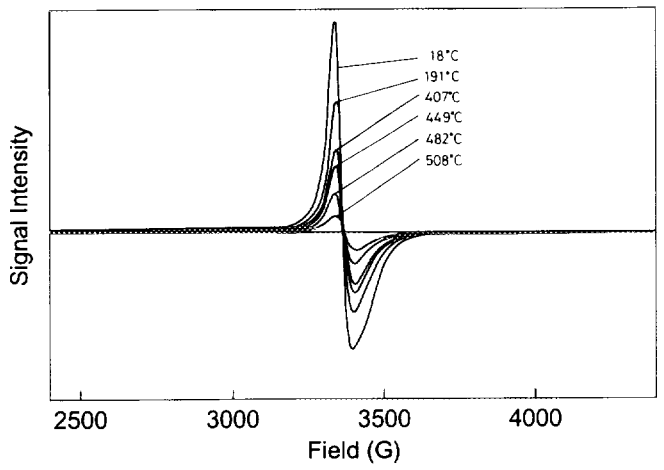


FIG. 7. ESR spectra of the V(IV) compound $Na_2VO(SO_4)_2$ measured at different temperatures in air.

work. A continuous decrease in the signal intensity is observed for all compounds, in accordance with the change in the Boltzmann distribution and the $Q$ value of the ESR cavity caused by increasing temperature. Except for $Na_2VO(SO_4)_2$, as shown in Fig. 7, the features of the spectra ($g$ values, anisotropy/isotropy) remain unchanged during the heating. For $Na_2VO(SO_4)_2$ the spectra change from anisotropic to almost isotropic, indicating that a solid–solid phase transition takes place. This change is clearly seen in Fig. 8, where the spectra have been double integrated, corrected for the change in the Boltzmann distribution and $Q$ value of the cavity, and finally normalized. The values from several spectra, which for reasons of clarity, were not shown in Fig. 7, are included here. Only for $Na_2VO(SO_4)_2$ is a jump in the relative signal intensity observed during the heating at around 300°C, well below the decomposition temperature. This temperature is in the range 450–500°C, as judged from the onset of the loss of signal intensity. It should be noted that the measurements have been performed by stepwise increase in the temperature about every 15 min. Thus, the measurements above the onset temperature of decomposition do not correspond to fully equilibrated samples, which of course would have shown zero signal intensity, characteristic of the ESR-silent V(V) complexes. After the decomposition, the initial blue color of the samples was transformed to dark reddish brown, which is typical for V(V) compounds.

It should be noted that for V(III) compounds the decomposition temperature has been found to be somewhat higher, even in an oxidizing atmosphere (5). Thus, to secure a complete activity restoration of deactivated catalysts, a heat treatment at around 500°C in an oxidizing atmosphere seems to be necessary.

## CONCLUSIONS

Industrial $SO_2$ oxidation catalysts and their molten salt–gas model systems $M_2S_2O_7/V_2O_5$–$SO_2/O_2/SO_3/N_2$ ($M$ = Na, K, Cs) have been investigated by combined measurements of their catalytic activity and ESR spectra. A 10% $SO_2$, 11% $O_2$, and 79% $N_2$ standard feed gas was used at 0%, 50%, or 90% preconversion, thus reflecting the conditions in an industrial converter from the first to the last catalyst bed. Below a certain temperature, the catalytic activity decreases and, simultaneously, vanadium compounds in reduced oxidation states precipitate. Table 3 lists these possible catalyst deactivation products.

A series of ESR spectra of the V(IV) compounds has been obtained and it is shown by *in situ* ESR measure-

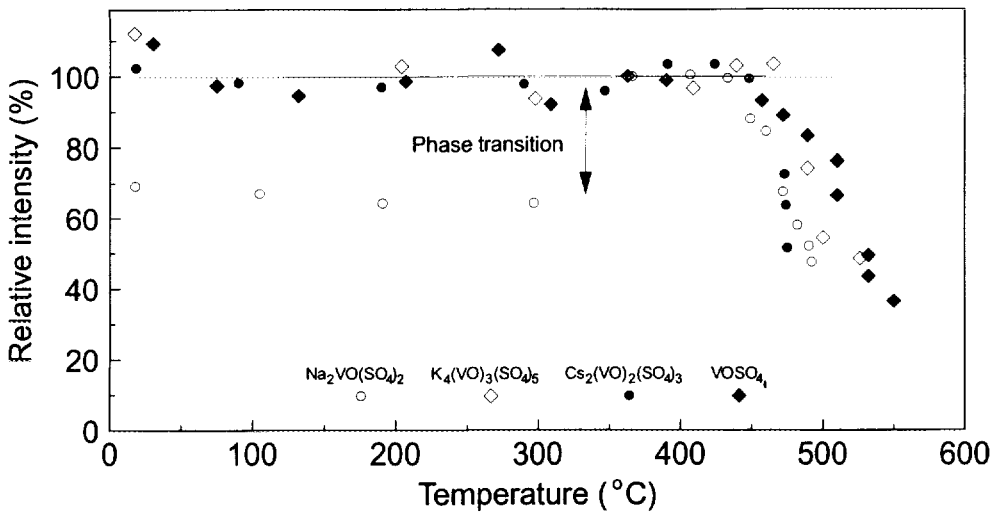


FIG. 8. Relative intensity of the ESR spectra of the V(IV) compounds vs temperature.

TABLE 3

**Possible Compounds Responsible for Catalyst Deactivation**[a]

| V(IV) | | V(III) | |
|---|---|---|---|
| $Na_2VO(SO_4)_2$ | (36) | $NaV(SO_4)_2$ | (37) |
| $Na_3(VO)_2(SO_4)_4$[b] | (28) | $Na_3V(SO_4)_3$ | (38) |
| $K_4(VO)_3(SO_4)_5$ | (39) | $KV(SO_4)_2$ | (40) |
| $K_3(VO)_2(SO_4)_4$[b] | (30) | | |
| $Cs_2(VO)_2(SO_4)_3$ | (41) | $CsV(SO_4)_2$ | (42) |
| $\beta$-$VOSO_4$ | (43) | | |
| $VOSO_4(SO_2SO_3)_x$[c] | (29) | | |

[a] The references include the crystal structure and the spectroscopic characterization of the compounds.

[b] Mixed valence V(IV)–V(V) compounds.

[c] $VOSO_4$-like lattice with incorporated $SO_2$ and/or $SO_3$ molecules.

ments of industrial catalysts how useful this information might be for the diagnosis of catalyst deactivation.

The temperature of deactivation is lowered by increasing the partial pressure ratio $P_{SO_3}/P_{SO_2}$, in accordance with a shift of the vanadium complex equilibria from the reduced oxidation states, V(III) and V(IV), to the highest oxidation state, V(V). In addition, the low temperature catalytic activity increases by

—increased atomic number of the alkali promoter,
—mixing of the alkali promoters, and
—dilution of the melt with respect to vanadium (which, however, decreases the overall activity).

From the temperature dependence of the ESR spectra of the V(IV) compounds, the temperature of decomposition and reoxidation is found to be in the range 450–500°C. A heat treatment at around 500°C in an oxidizing atmosphere seems to be necessary for the reactivation of deactivated catalysts.

This investigation has been carried out in order to obtain detailed information about the severe deactivation of industrial catalysts and give inspiration for the design of modified catalysts with improved low-temperature activity. The aim of future investigations should be to elucidate the details of the reaction mechanism explaining why the catalyst is active, i.e., a thorough study of the formation of vanadium complexes and their interaction with the gaseous reactants and products.

## ACKNOWLEDGMENTS

This investigation has been supported by the EEC programs BRITE-EURAM II (contract BRE2.CT93.0447) and Human Capital and Mobility (contract ERBCHBGCT920129) and the Danish Natural Science Research Council. A. Chrissanthopoulos is thanked for experimental assistance and G. N. Papatheodorou for helpful discussions.

## REFERENCES

1. Frazer, J. H., and Kirkpatrick, W. J., *J. Am. Chem. Soc.* **62,** 1659 (1940).
2. Topsøe, H. F. A., and Nielsen, A., *Trans. Dan. Acad. Tech. Sci.* **1,** 18 (1947).
3. Villadsen, J., and Livbjerg, H., *Catal. Rev.-Sci. Eng.* **17,** 203 (1978).
4. Kenney, C. N., *Catal. Rev.-Sci. Eng.* **11,** 197 (1975).
5. Boghosian, S., Fehrmann, R., Bjerrum, N. J., and Papatheodorou, G. N., *J. Catal.* **119,** 121 (1989).
6. Nielsen, K., Fehrmann, R., and Eriksen, K. M., *Inorg. Chem.* **32,** 4825 (1993).
7. Karydis, D. A., Eriksen, K. M., Fehrmann, R., and Boghosian, S., *J. Chem. Soc. Dalton Trans.*, 2151 (1994).
8. Grydgaard, P., Jensen-Holm, H., Livbjerg, H., and Villadsen, J., *ACS Symp. Ser.* **65,** 582 (1978).
9. Eriksen, K. M., Fehrmann, R., and Bjerrum, N. J., *J. Catal.* **132,** 263 (1991).
10. Mastikhin, V. M., Polyakova, G. M., Zyulkovski, Y., and Boreskov, G. K., *Kinet. Katal.* **11,** 1463 (1970); *Kinet. Catal. Engl. Transl.* **11,** 1219 (1970).
11. Boreskov, G. K., Davydova, L. P., Mastikhin, V. M., and Polyakova, G. M., *Dokl. Akad. Nauk. SSSR* **171,** 648 (1966); *Dokl. Akad. Nauk. SSSR Engl. Transl.* **171,** 760 (1966).
12. Boreskov, G. K., Polyakova, G. M., Ivanov, A. A., and Mastikhin, V. M., *Dokl. Akad. Nauk. SSSR* **210,** 626 (1973).
13. Doering, F. J., and Berkel, D., *J. Catal.* **103,** 126 (1987).
14. Doering, F., Yuen, H. K., Berger, P. A., and Unland, M. L., *J. Catal.* **104,** 186 (1987).
15. Hansen, N. H., Fehrmann, R., and Bjerrum, N. J., *Inorg. Chem.* **21,** 744 (1982).
16. Folkmann, G. E., Hatem, G., Fehrmann, R., Gaune-Escard, M., and Bjerrum, N. J., *Inorg. Chem.* **30,** 4057 (1991).
17. Folkmann, G. E., Ph.D. Thesis, Technical University of Denmark, Lyngby, 1991.
18. Karydis, D. A., Boghosian, S., and Fehrmann, R., *J. Catal.* **145,** 312 (1994).
19. Tandy, G. H., *J. Appl. Chem.* **6,** 68 (1956).
20. Spitsyn, V. I., and Mikhailenko, I. E., *J. Inorg. Chem. USSR* **2,** 2416 (1957).
21. Flood, H., and Førland, T., *Acta Chem. Scand.* **1,** 781 (1947).
22. Mars, P., and Maessen, J. G. H., *in* "Proceedings, 3rd International Congress on Catalysis. Amsterdam, 1964," Vol. 1, p. 266. 1965; *J. Catal.* **10,** 1 (1968).
23. Xie, K. C., and Nobile, A. J., *J. Catal.* **94,** 323 (1985).
24. Livbjerg, H., and Villadsen, J., *Chem. Eng. Sci.* **27,** 21 (1972).
25. Ibers, J. A., and Swalen, J. D., *Phys. Rev.* **127**(6), 1914 (1962).
26. Krasil'nikov, V. N., Glazyrin, M. P., Palkin, A. P., Perelyaeva, L. A., and Ivakin, A. A., *Zh. Neorg. Khim.* **32,** 760 (1987); *Russ. J. Inorg. Chem. Engl. Transl.* **32**(3), 425 (1987).
27. Krasil'nikov, V. N., and Krivchenko, Yu. I., *Zh. Prik. Khim.* **62,** 444 (1989); *J. Appl. Chem. USSR Engl. Transl.* **62,** 402 (1989).
28. Oehlers, C., Nielsen, K., Eriksen, K. M., and Fehrmann, R., in preparation.
29. Nielsen, K., et al. In preparation.
30. Eriksen, K. M., Nielsen, K., and Fehrmann, R., submitted for publication.
31. Belford, R. L., Chasteen, N. D., So, H. and Tapscott, R. E., *J. Am. Chem. Soc.* **91,** 4675 (1969).
32. Toftlund, H., Larsen, S. and Murray, K. S., *Inorg. Chem.* **30,** 3964 (1991).
33. Dickinson, L. C., Dunhill, R. H., and Symons, M. C. R., *J. Chem. Soc. A*, 922 (1970).
34. Karydis, D. A., Eriksen, K. M., Fehrmann, R., Papatheodorou, G. N., and Bjerrum, N. J., *Mater. Sci. Forum* **73–75,** 115 (1991).

35. Boreskov, G. K., and Sogam, S. M., *Zh. Fiz. Khim.* **14,** 1337 (1940).
36. Fehrmann, R., Boghosian, S., Papatheodorou, G. N., Nielsen, K., Berg, R. W., and Bjerrum, N. J., *Inorg. Chem.* **29,** 3294 (1990).
37. Fehrmann, R., Boghosian, S., Papatheodorou, G., N., Nielsen, K., Berg, R. W., and Bjerrum, N. J., *Acta Chem. Scand.* **45,** 961 (1991).
38. Boghosian, S., Fehrmann, R., and Nielsen, K., *Acta Chem. Scand.* **48,** 724 (1994).
39. Fehrmann, R., Boghosian, S., Papatheodorou, G. N., Nielsen, K., Berg, R. W., and Bjerrum, N. J., *Inorg. Chem.* **28,** 1847 (1989).
40. Fehrmann, R., Krebs, B., Papatheodorou, G. N., Berg, R. W., and Bjerrum, N. J., *Inorg. Chem.* **25,** 1571 (1986).
41. Boghosian, S., Nielsen, K., and Fehrmann, R., in preparation.
42. Berg, R. W., Boghosian, S., Bjerrum, N. J., Fehrmann, R., Krebs, B., Strater, N., Mortensen, O. S., and Papatheodorou, G. N., *Inorg. Chem.* **32,** 4714 (1993).
43. (a) Kierkegaard, P., and Longo, J. M., *Acta Chem. Scand.* **19,** 99 (1965); (b) Nielsen, K., Boghosian, S., Eriksen, K. M., and Fehrmann, R. *Acta Chem. Scand.* **49,** (1995), in press.